ARTICLES
PUBLISHED ONLINE: 25 JANUARY 2016 | DOI: 10.1038/NNANO.2015.324
nature nanotechnology

A transparent bending-insensitive pressure sensor

Sungwon Lee[1,2], Amir Reuveny[1,2], Jonathan Reeder[1†], Sunghoon Lee[1,2], Hanbit Jin[1,2], Qihan Liu[3], Tomoyuki Yokota[1,2], Tsuyoshi Sekitani[1,2,4], Takashi Isoyama[5], Yusuke Abe[5], Zhigang Suo[3] and Takao Someya[1,2*]

Measuring small normal pressures is essential to accurately evaluate external stimuli in curvilinear and dynamic surfaces such as natural tissues. Usually, sensitive and spatially accurate pressure sensors are achieved through conformal contact with the surface; however, this also makes them sensitive to mechanical deformation (bending). Indeed, when a soft object is pressed by another soft object, the normal pressure cannot be measured independently from the mechanical stress. Here, we show a pressure sensor that measures only the normal pressure, even under extreme bending conditions. To reduce the bending sensitivity, we use composite nanofibres of carbon nanotubes and graphene. Our simulations show that these fibres change their relative alignment to accommodate bending deformation, thus reducing the strain in individual fibres. Pressure sensitivity is maintained down to a bending radius of 80 μm. To test the suitability of our sensor for soft robotics and medical applications, we fabricated an integrated sensor matrix that is only 2 μm thick. We show real-time (response time of ~20 ms), large-area, normal pressure monitoring under different, complex bending conditions.

The accurate real-time measurement of vital information using electronic sensors in a living body is important for health monitoring and medical applications[1,2]. Most tissue surfaces, whether internal or external, are inherently soft and constantly in motion. Thus, sensors that directly touch the surface of a living body should ideally be soft so as to establish good mechanical contact between the electronic device and biological tissue. To realize soft sensors, significant effort has recently been made to manufacture electronic devices on soft substrates such as plastic and rubber[3–7]. Examples of mechanically flexible electronic devices include pressure[8–10], temperature[11] and strain sensors[9,10], as well as two-dimensional multi-electrode arrays for sensing electrical signals from the body[12,13].

Pressure measurements, in particular, require direct contact between the sensor and target object, so flexible pressure sensors are indispensable when a target is soft. As a result of recent progress in flexible electronic technologies, flexible pressure sensors have been developed with improved sensitivity, accuracy, reliability and level of integration[14–21]. The sensitivity of flexible pressure sensors has been significantly improved using unique elastic pyramid-shaped microstructures[14] or a nanofibre interlocking system with a high-aspect-ratio vertical achitecture[9]. The best sensitivity reported is 56–133 kPa^{-1} in the pressure regime below 30 Pa (ref. 17). Furthermore, the conformability and/or mechanical flexibility of pressure sensors have been improved by reducing the thickness of sensing elements based on piezoelectric materials down to 300 nm and that of elastomer substrates down to 20 μm (ref. 21).

Despite the good performance and high flexibility of these devices, the accurate measurement of pressure under dynamic deformation has remained difficult because the sensing properties vary significantly as a result of the strains induced by mechanical deformation (such as bending, twisting and wrinkling). When elastic materials are used as substrates or sensing elements to achieve high pressure sensitivity and good conformability, a large lateral strain is inevitably induced by bending because of their large Young's moduli. In contrast, when flexible pressure sensors (either resistive or capacitive) are manufactured on plastic foils, the strains induced by bending and other associated complexities will be suppressed by a reduction in the total thickness of all components. However, reducing the scale of sensing elements, such as the elastic conducting materials, down to the micrometre scale or lower remains challenging. Although elastic conductors have been realized by mixing conductive nanofillers such as carbon nanotubes (CNTs) with fluorinated copolymers[22,23], their thickness typically remains 100 μm or larger because of the difficulties in achieving uniform mixing. Furthermore, elastic conductors are designed to exhibit a large conductivity without applying pressure, so highly conductive materials show a very small change in conductivity when pressure is applied. Hence, a new material design concept that does not involve elastic conductors is required to realize flexible pressure sensors that can accurately measure only the normal pressure on complex and moving surfaces.

In this Article, we report the fabrication of extraordinarily small bending-sensitive, ultra-flexible, optically transparent and resistive-type pressure sensors using composite nanofibres. To minimize the rigidity and total thickness of our pressure sensors we used an electrospinning process[24]. Because of the nanoporous structure, the sensors exhibited an extremely small sensitivity to the bending-induced strain, while maintaining a high sensitivity and excellent conformability to three-dimensional structures. Indeed, when the sensors were bent to a bending radius as low as 80 μm, the sensor properties remained practically unchanged. Our bending-insensitive device was used to accurately measure the distribution of the normal pressure (without suffering from the inaccuracy induced by mechanical deformations such as wrinkling and twisting) on the soft movable three-dimensional surface of a balloon that was being pressed by a soft object such as a finger.

[1]Department of Electrical and Electronic Engineering, The University of Tokyo, 7-3-1 Hongo, Bunkyo-ku, Tokyo 113-8656, Japan. [2]Exploratory Research for Advanced Technology (ERATO), Japan Science and Technology Agency (JST), 7-3-1 Hongo, Bunkyo-ku, Tokyo 113-8656, Japan. [3]Kevli Institute of Bionano Technology and Science, John A, Paulson School of Engineering and Applied Sciences, Harvard University, Cambridge, Massachussetts 02138, USA. [4]The Institute of Scientific and Industrial Research, Osaka University, 8-1 Mihogaoka, Ibaraki, Osaka 567-0047, Japan. [5]Graduate School of Medicine, The University of Tokyo, 7-3-1 Hongo, Bunkyo-ku, Tokyo 113-0033, Japan. †Present address: Department of Materials Science and Engineering, The University of Texas at Dallas, Richardson, Texas 75080, USA. *e-mail: someya@ee.t.u-tokyo.ac.jp

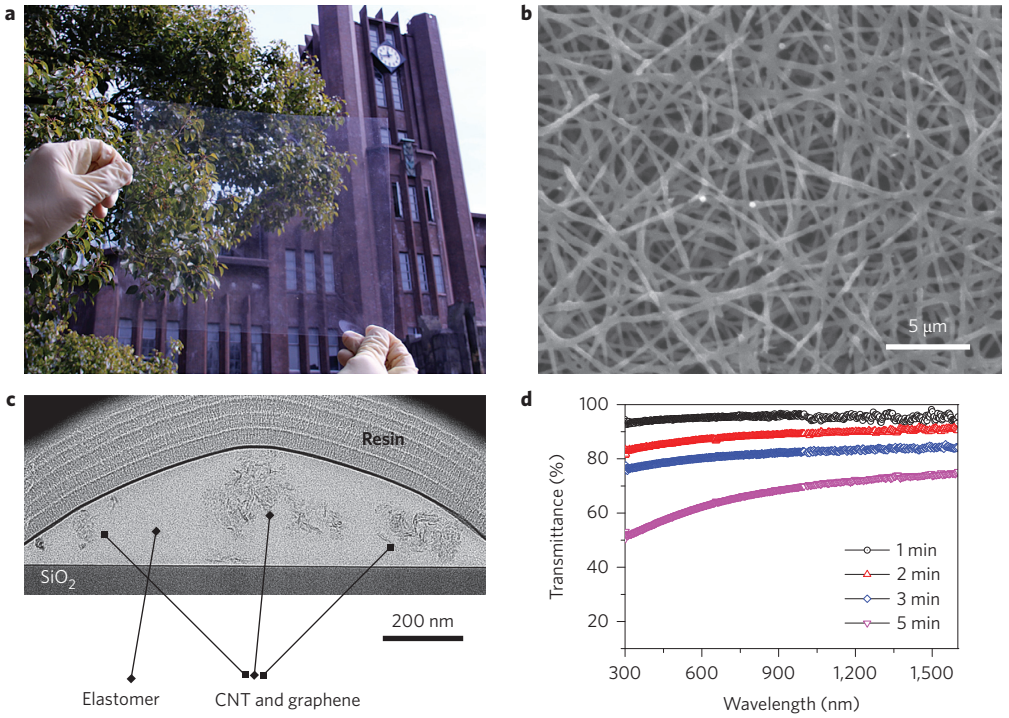

Figure 1 | Transparent pressure-sensitive nanofibre. a, Photograph of large-area-deposited nanofibres using electrospinning on a transparent polymer film (25×20 cm^2), showing excellent transparency. **b**, FESEM image of the randomly stacked electrospun nanofibres (diameter of 300–600 nm). **c**, Cross-sectional image of a single pressure-sensitive nanofibre observed by HRTEM, indicating good dispersion of the CNTs and graphene in the elastomer nanofibre matrix. **d**, Measured transmittance as a function of light wavelength from 300 to 1,600 nm for different deposition times.

Fabrication of bending-insensitive nanofibre composite

The ultrathin, bending-insensitive and optically transparent pressure sensor was manufactured using pressure-sensitive nanofibres. The uniform dispersion of conducting nanomaterials (CNTs and graphene) inside the nanofibres was strategically designed to create large sensing capabilities for each element to improve the sensing ability and facilitate downscaling. The nanofibres were fabricated by an electrospinning process using a composite material solution (Supplementary Fig. 1). The solution was composed mainly of a fluorinated copolymer, which acts as a nanofibre matrix. Small quantities of CNTs and graphene particles (0.017 and 1.7 wt%, respectively) were dispersed as conductive fillers. An ionic liquid was also added as a dispersing agent to prevent aggregation of the conductive fillers. Graphene was introduced to improve the pressure sensitivity, as will be described in the last section of this article. Figure 1a shows the uniformly dispersed optically transparent nanofibre layer on a polymer substrate (deposition time of 1 min). Despite the use of a black conductive filler, we achieved transparency owing to the thinness of the layer (~2 μm) and its porosity. The thickness was defined as the average value of the laterally profiled height of the deposited fibres. The deposited electrospun fibre layer is extremely light (~50 mg m^{-2}) and flexible, similar to a spider web. Accordingly, the pressure-sensitive material does not significantly affect the device flexibility and total weight, which are critical features in realizing conformal no-stress contact on skin or living organs.

The structure of the pressure-sensitive nanofibre layer was characterized using field-emission scanning electron microscopy (FESEM; Fig. 1b). The diameters of the nanofibres were observed to fall within the range 300–700 nm. Several layers of fibres were randomly entangled and stacked to form a porous structure. High transparency and high pressure sensitivity were achieved because of the porous structure and the small diameter of each fibre, as will be explained in the last section. A cross-section of a single fibre was examined using high-resolution transmission electron microscopy (HRTEM), and the graphene and CNTs were found to be dispersed in the elastomer matrix with small aggregations (Fig. 1c and Supplementary Fig. 2).

The electrical properties and optical transparency of the electrospun fibre can be controlled by changing the deposition time, because the density and effective thickness of the deposited layer increase with deposition time. Four samples were prepared on glass substrates with different deposition times of 1, 2, 3 and 5 min, and their transmittances were compared (Supplementary Fig. 3). For 1 min of electrospinning deposition, the transmittance exceeded 90% in the visible-to-infrared wavelength region (300–1,600 nm). Such a high optical transparency is a useful feature for integration with optical devices such as displays and bio-imaging devices[25]. The transmittance decreased by ~10% when the deposition time was increased by 1 min (Fig. 1d). The average thickness slightly increased from 2 to 3 μm (for an area of 20×20 cm^2) with increasing deposition time.

Electrical characteristics of the sensor under bending

The sensitivity of the pressure sensors was greatly enhanced by using the nanofibre stacking structure compared with sensors fabricated using a conventional thin-film structure. The nanofibrous sensors were fabricated by depositing nanofibres for 1 min between 40-nm-thick Au electrodes (1 cm^2) coated on poly(ethylene terephthalate) (PET) substrates. For comparison, the same composite materials used for the nanofibre sensors were deposited using screen-printing to form a thin continuous film with a thickness of 20 μm, which was sandwiched between two electrodes (a design referred to as a thin-film sensor). Figure 2a shows the response to pressure up to 10 kPa. Magnified data for pressures from 0 to 1 kPa (for the same results) are shown in the inset. The resistance of the nanofibre sensor was 6 GΩ without any applied pressure, which is a factor of 1×10^5 higher than that of the thin-film sensor, although the average thickness of the former was smaller by a factor of ~10. The resistance of the nanofibrous sensors

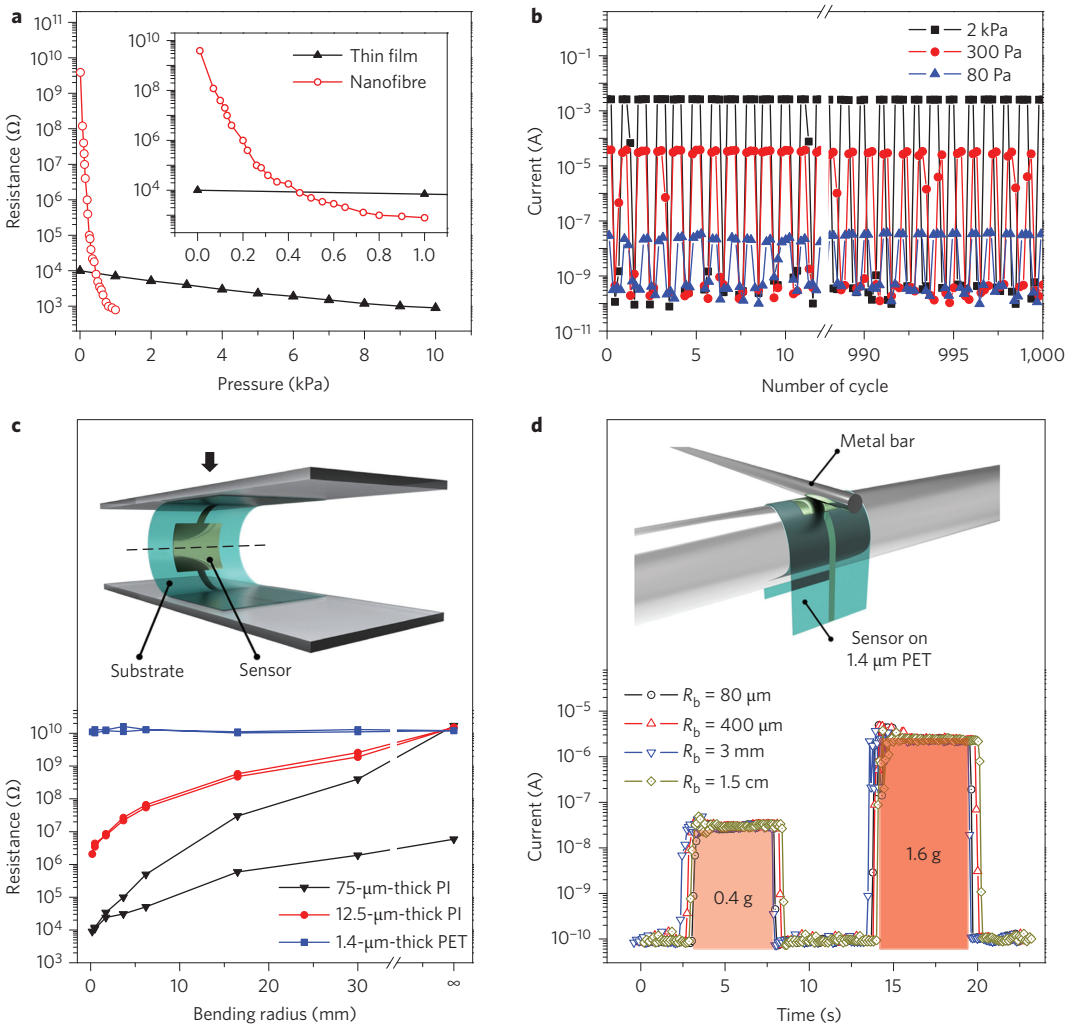

Figure 2 | Electrical properties of a pressure-sensitive nanofibre and performance under bending. a, Pressure versus resistance curve of the nanofibre sensor (red) and thin-film sensor (black) sandwiched between Au electrodes (1×1 cm^2; the inset represents the pressure from 0 to 1 kPa). **b**, On/off cyclic test of the sensor over the initial ten and final ten cycles at different pressures. **c**, Schematic showing the pressure response measurement of the sensor under bending and response curves when bent to a radius of 180 μm for different substrate thicknesses. **d**, Tested pressure response of the device in the bent state and response of the device fabricated on a 1.4-μm-thick PET substrate for a bending radius from 15 mm to 80 μm for different normal forces (0.4 or 1.6 g).

decreased drastically with application of a very small pressure (~800 Pa), falling below 1×10^3 Ω. In contrast, the resistance of the thin-film sensors changed by only a factor of 10 with application of 10 kPa of pressure. This extremely large change (by a factor of over 1×10^6) exhibited by the nanofibrous sensors enables the easy detection of very small pressure signals such as those from biological tissues. The excellent uniformity of this sensing characteristic was confirmed for an effective area of 9×9 cm^2 (Supplementary Fig. 4 and Supplementary Movie 1).

To evaluate the reversibility and reproducibility of the pressure sensor, we conducted cycle tests by applying and releasing pressure of 2,000, 300 and 80 Pa, with 1,000 repetitions for each pressure, using the same device (Supplementary Fig. 5). The initial ten and final ten cycles are shown in Fig. 2b. The on/off ratio was constant throughout the test, showing reproducible and reliable pressure detection. The response times of the device were ~20 and 5 ms when the pressure was applied and released, respectively, which should be sufficiently fast for many biomedical applications (Supplementary Fig. 6).

We examined the effect of the bending-induced strain on the performance of the pressure sensors. Three samples with a pad area of 1 cm^2 were prepared using the same nanofibre layers on different substrates, namely, 75-μm-thick polyimide (PI), 12.5-μm-thick PI and 1.4-μm-thick PET substrates. Figure 2c shows that the sensors were bent, reducing the bending radius to 180 μm, and then returned to their original, flat state (Supplementary Fig. 7a,b). The resistance response to the mechanical bending of each device was measured during the bending. We note that the device fabricated on a 1.4-μm-thick PET substrate exhibited negligible resistance changes during the bending test. In sharp contrast, the resistance of the devices fabricated on both 75- and 12.5-μm-thick PI substrates decreased approximately linearly until the bending radius reached 20 mm. A further reduction in the bending radius caused severe changes in the resistance or resulted in irreversible degradation (Supplementary Fig. 7c).

To separately measure the normal pressure from the strain by deformation on a three-dimensional surface, the pressure difference between the bent and flat sensors must be negligibly small. We therefore measured the response to pressure of the device fabricated on the 1.4-μm-thick film while the bending radius was varied. A schematic of the measurement set-up is shown in the inset to Fig. 2d, and the features of the extremely bent device and other information are shown in Supplementary Fig. 8. The device performance was evaluated at bending radii of 1.5 cm, 3 mm, 400 μm and 80 μm. Pressure was applied to the sensor area using a small

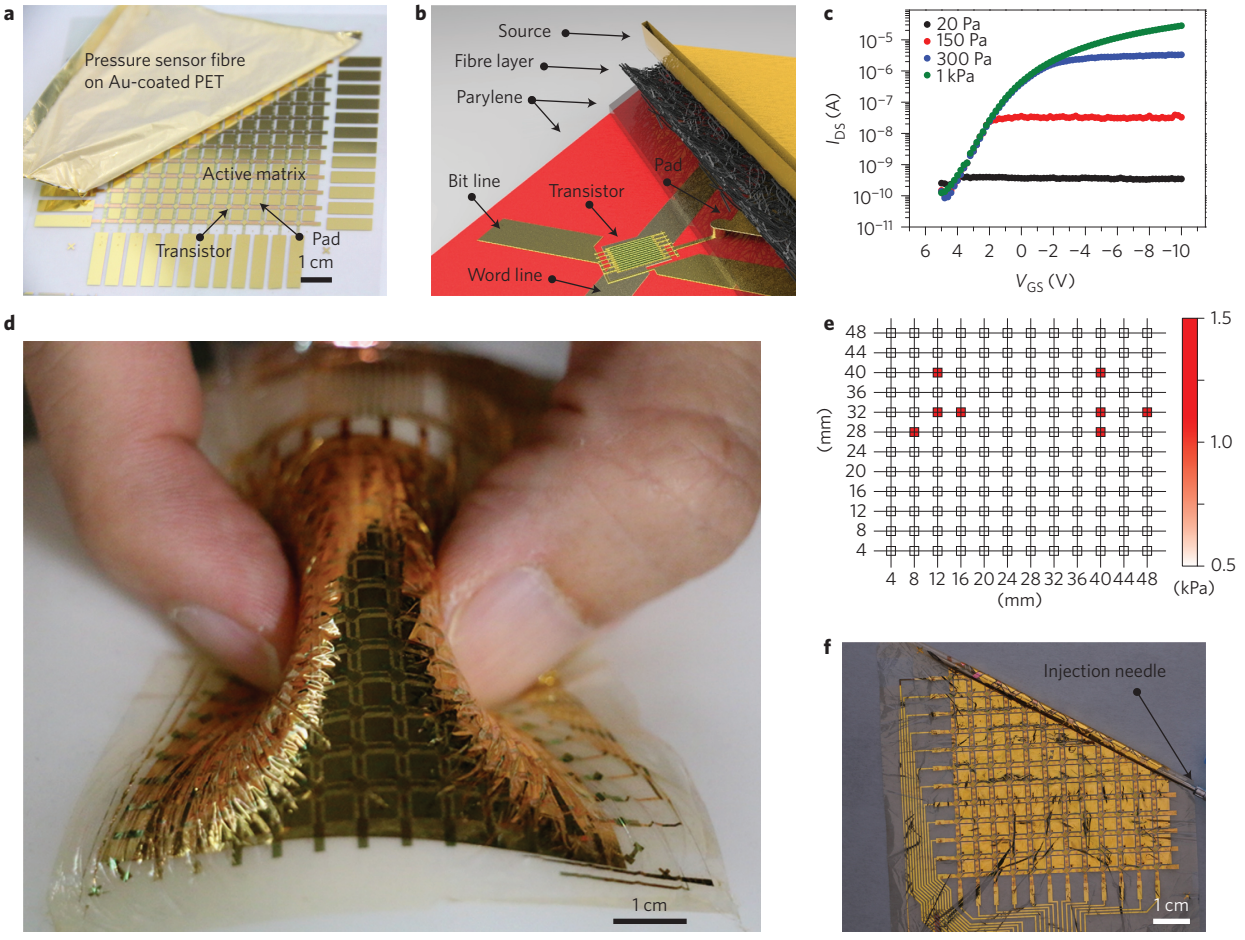

Figure 3 | Pressure-sensor integration with an organic-transistor-driven active matrix. a, Photograph of the active matrix (12 × 12 pixels) integrated with a large-area (9 × 9 cm^2) pressure-sensor nanofibre sheet. **b**, Schematic of a single-sensor pixel. **c**, Representative transfer-curve behaviour of a single pixel at different applied pressures, showing the large sensitivity and low-voltage operation. **d**, Photograph of an integrated sensor array attached to the surface of a soft balloon, to which a pressure was applied by a pinching motion. **e**, Measured pressure data distribution under complex bending, showing no pressure signal from deformation such as wrinkling. **f**, Photograph of a sensor wrapped around an injection needle.

metal rod (0.8 or 3.2 g). The applied stimulus was denoted as a mass because the contact area was not well defined. We thus present the response of the device only to different normal forces The response to pressure application, that is, the relative change in the current and response time, remained essentially unchanged (less than 20% variation in the absolute current values) for all four bending radii. The current was ~100 pA with no applied pressure. The response times (<20 ms) and pressure responses were nearly identical under the various normal forces, as shown in Fig. 2d. Our device did not experience any mechanical or electrical failure during the extreme bending process because of the thin substrate and entangled nanostructure. The pressure response at a bending radius of 80 μm is shown in Supplementary Movie 2.

Real-time pressure distribution under complex deformation

The novelty of our bending-insensitive sensors is particularly important when the target objects are soft movable three-dimensional surfaces. Indeed, in the past, when a soft object was pressed by another soft object, the normal pressure could never be measured separately from the mechanical stress. To demonstrate this capability we fabricated a 12 × 12 ultrathin pressure-sensor matrix with a total thickness of 8 μm by integrating our nanofibre sensors with an active matrix with a thickness of 2 μm (including the substrate and encapsulation; Fig. 3a,b). Similar ultra-thin active matrices have been used with interdigitated metallic and gel electrodes for ultra-thin touch sensors[26] and electrocardiography[27] for biological applications because of their excellent conformability. The device was then applied to the very soft surface of a balloon. The representative transfer curves at different pressures are shown in Fig. 3c. The characteristics of the matrix and other details are provided in Supplementary Fig. 9. Owing to the soft nature of both the balloon and finger, our device was deformed by complex bending and severe wrinkling. To induce a substantially large deformation to the balloon, a pressure larger than the minimum sensitivity of our device was applied by pinching with two fingers. However, because of the ultra-thin format of the device and its bending insensitivity, we successfully measured only the normal pressure distribution on the balloon (a soft target) resulting from the application of pressure by fingers (soft objects). The applied pressure (~0.6–1.5 kPa) was successfully monitored in a three-dimensional configuration that included complex bending and wrinkling between soft materials (Fig. 3d,e). More mapping and video data are presented in Supplementary Fig. 10 and Supplementary Movie 3). The nanofibrous sensor arrays can also be used on the surface of human skin to measure the pressure distribution (Supplementary Fig. 11). The crosstalk between the 1-mm-spacing sensor arrays is negligibly small, as shown in Supplementary Fig. 12.

We also took advantage of the bending insensitivity to wrap fully integrated devices around an injection needle with a bending radius of 1 mm (Fig. 3f), and the changes in performance were found to be negligibly small before and after wrapping. The current level was below 300 pA, which represents an insignificant pressure.

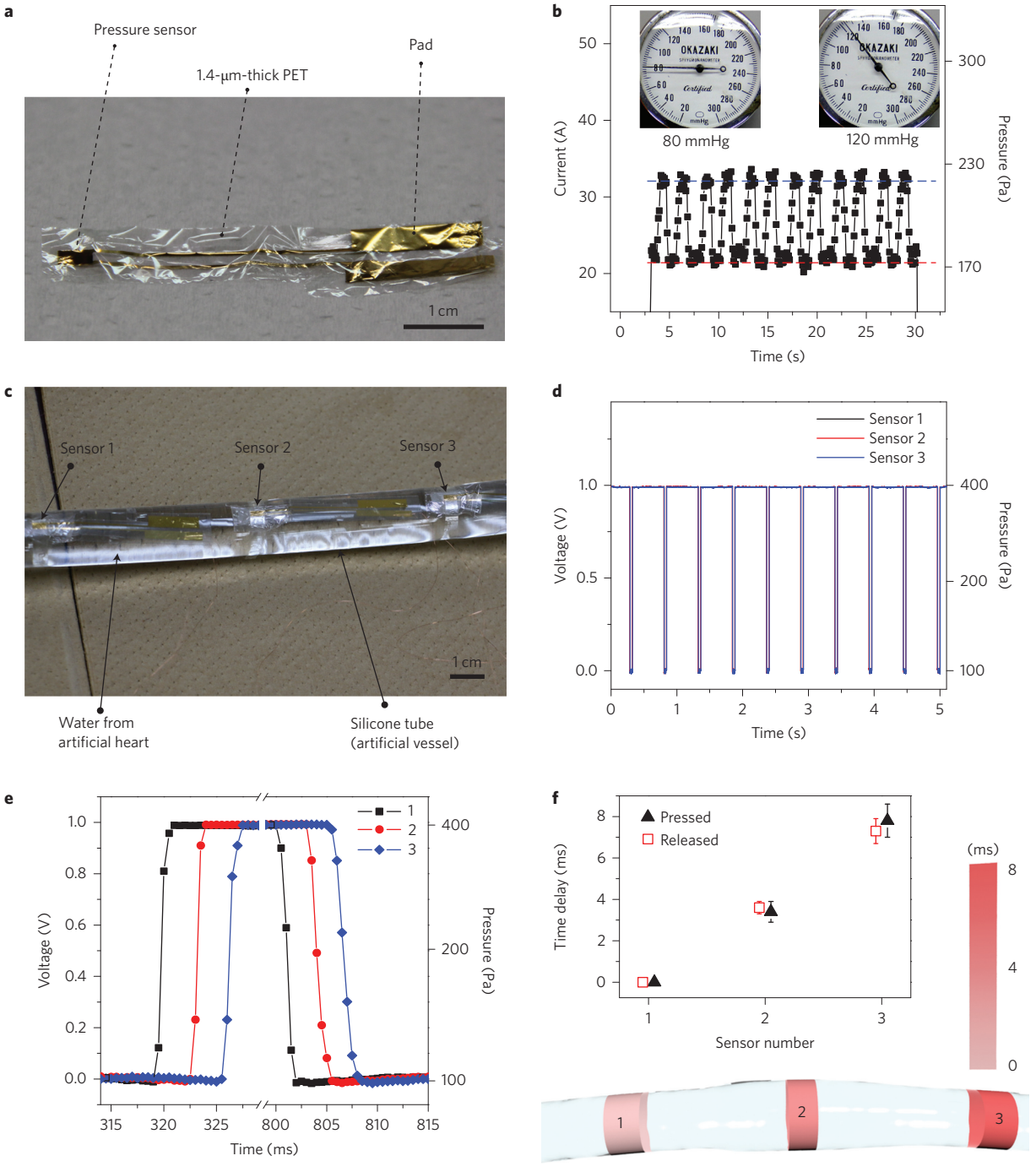

Figure 4 | Measurement of pressure propagation speed in an artificial cardiac system. a, Photograph of a small pressure sensor (2×4 mm^2). **b**, Cyclic test of the pressure response from a single sensor (80 or 120 mmHg) attached to an artificial blood vessel. **c**, Experimental set-up for measuring the pressure propagation from the artificial blood vessel. **d**, Simultaneous measurement of the pressure from three sensors attached to the vessel. **e**, Representative pressure response from a single pressure wave, showing the time delay according to the location of the sensors. **f**, Average time delay of the response between sensors and the standard deviation from ten pressure waves.

Additionally, the sensing range and sensitivity of the device can be easily controlled for various applications by controlling the following parameters: thickness of the fibre layer (Supplementary Fig. 13), concentration of the conductive filler in the fibre, pad size and width/length (W/L) ratio of the transistors. The mechanical robustness of the device was tested by measuring the pressure response before and after severely crumpling it ten times. The pressure response of a representative pixel was monitored, and we found almost no performance change after repeated large deformation (Supplementary Fig. 14).

The sensor was also applied to an artificial cardiac system. A silicone tube was used as a blood-vessel model, with similar mechanical properties such as the expansion ratio (modulus). A small pressure sensor (2×4 mm^2, Fig. 4a) was attached to the tube and wrapped by a polymer film to detect the vessel expansion. The sensor structure and experimental set-up are provided in Supplementary Fig. 15. The pressure was measured while air pressure was applied inside the tube (Fig. 4b). Despite the very small volume change in the artificial blood vessel (outer diameter of 18 mm) and its small bending radius, our device successfully detected the cyclic change in pressure

(50 Pa). Next, we applied three sensors on a vessel with a 6 cm spacing to detect the speed of pressure propagation (Fig. 4c and Supplementary Fig. 16). Water pressure was applied using a displacement-type artificial heart system. The measured voltage data from the three sensors showed excellent agreement in response to the pressure changes and a clear delay time could be observed at the sub-millisecond scale (Fig. 4d,e) depending on the location of the sensor (sensor 1 was closest to the pump). The average time delay between sensors was ~3.5 ms (Fig. 4f), indicating a speed of pressure propagation of ~17.1 m s^{-1} in this system. The development of sophisticated encapsulation is expected to improve the stability of the device for *in vivo* measurements.

Pressure sensitivity and bending insensitivity mechanism

To understand the function of the CNTs in the CNT/graphene mixture, it was interesting to compare the results for three different samples (a fluorinated copolymer with only CNTs, one with only graphene, and one with the CNT/graphene mixture). The sample consisting of the copolymer with only CNTs (1 wt%) exhibited a low resistance (over 1×10^6 Ω), and the resistance reduced by two orders of magnitude when a pressure of 1 kPa was applied (Fig. 17). This could be used as a sensor, but improvements in its sensitivity are desirable. In sharp contrast, the sample consisting of the copolymer with only graphene (1.7 wt%) exhibited a very high resistance (over 1×10^8 Ω) and the high resistance was maintained even when a pressure up to 10 kPa was applied. This is neither a sensor nor a conductor. In Fig. 2a it is noteworthy that, when a small number of CNTs (0.017 wt%) is added to the sample consisting of the copolymer with only graphene (1.7 wt%), the resistance is high (1×10^{10} Ω) without pressure, and it exhibits an extraordinarily large change in the resistance when a small pressure is applied. These experiments unambiguously show that a very small number of CNTs—which are one-dimensional conductive fillers—efficiently form conductive paths between the graphene fillers with application of a very small pressure, realizing an extraordinarily large change in the resistance. Additionally, by using a nanofibrous structure, we can achieve an extraordinarily small sensitivity to the bending-induced strain while maintaining high sensitivity, transparency and excellent conformability.

The key to the success of the bending insensitivity is the adoption of a nanofibrous structure. The fibrous material changes the alignment and accommodates the deformation, thus reducing strain in the individual fibres (Supplementary Fig. 18), similar to a cellulous material, which is more flexible for deformation[28]. We illustrate the structural advantage of the fibrous material using a simulation, in which the fibrous material is represented by a periodic mesh subject to bending deformation. The degree of bending was measured by dividing the bending radius R by the thickness of the mesh t. We found that when $R/t = 2$, the majority of the fibres experienced less than 5% strain, and the maximum strain was ~7% (Supplementary Fig. 19a). The deformation is mostly accommodated by rotating and deflecting the fibres instead of stretching the fibres. For comparison, if such a sheet is made of a continuous material, the maximum strain in the sheet follows the analytical expression $\varepsilon = t/2R$. When $R/t = 2$, the maximum strain would be 25%. We found that a fibrous structure exhibited ~70% less bending-induced strain compared with the continuous counterparts. When the fibrous sensor layer is sandwiched between two electrodes, the bending insensitivity may degrade due to the coupling between the sensor layer and the electrodes (Supplementary Fig. 19b). If the electrodes are much stiffer than the sensor layer, each electrode is approximately inextensible. Consequently, the sensor layer may be strongly sheared. In contrast, if the electrodes are much more compliant than the sensor layer, the electrodes will follow the deformation of the sensor layer and the bending insensitivity is recovered. This change in behaviour due to the relative stiffness of the electrodes was experimentally verified by modulating the thickness and the material of the electrodes (Fig. 2c).

Conclusions

We have demonstrated a transparent and bending-insensitive pressure sensor fabricated using composite nanofibres, which exhibits an extremely small sensitivity to a bending-induced strain. Our sensor enables the accurate measurement of only the normal pressure without suffering from the inaccuracy induced by mechanical deformation. This simple yet challenging experiment should inspire other clinical and health-monitoring applications such as *in situ* digital monitoring of palpation for breast cancer.

Methods

Methods and any associated references are available in the online version of the paper.

Received 7 January 2015; accepted 11 December 2015; published online 25 January 2016

References

1. Abe, Y. *et al.* Physiological control of a total artificial heart: conductance- and arterial pressure-based control. *J. Appl. Phys.* **84,** 868–876 (1998).
2. Pang, C., Lee, C. & Suh, K.-Y. Recent advances in flexible sensors for wearable and implantable devices. *J. Appl. Polym. Sci.* **130,** 1429–1441 (2013).
3. Kim, D. H. *et al.* Dissolvable films of silk fibroin for ultrathin conformal bio-integrated electronics. *Nature Mater.* **9,** 511–517 (2010).
4. Kim, D. H. *et al.* Epidermal electronics. *Science* **333,** 838–843 (2011).
5. Jeong, J.-W. *et al.* Materials and potimized designs for human–machine interfaces via epidermal electronics. *Adv. Mater.* **25,** 6839–6849 (2013).
6. Sekitani, T. & Someya, T. Human-friendly organic integrated circuits. *Mater. Today* **14,** 398–407 (2011).
7. Kim, D. H. *et al.* Materials for multifunctional balloon catheters with capabilities in cardiac electrophysiological mapping and ablation therapy. *Nature Mater.* **10,** 316–323 (2011).
8. Lipomi, D. J. *et al.* Skin-like pressure and strain sensor based on transparent elastic films of carbon nanotubes. *Nature Nanotech.* **6,** 788–792 (2011).
9. Pang, C. *et al.* A flexible and highly sensitive strain-gauge sensor using reversible interlocking of nanofibres. *Nature Mater.* **11,** 795–801 (2012).
10. Someya, T. *et al.* A large-area, flexible pressure sensor matrix with organic field-effect transistors for artificial skin applications. *Proc. Natl Acad. Sci. USA* **101,** 9966–9970 (2004).
11. Hammock, M. L., Chortos, A., Tee, B. C.-k., Tok, J. B.-H. & Bao, Z. The evalution of electronic skin (e-skin): a brief history, design considerations, and recent progress. *Adv. Mater.* **25,** 5997–6038 (2013).
12. Viventi, J. *et al.* Flexible, foldable, actively multiplexed, high-density electrode array for mapping brain activity *in vivo*. *Nature Neurosci.* **14,** 1599–1605 (2011).
13. Xu, L. *et al.* 3D multifunctional integumentary membranes for spatiotemporal cardiac measurements and stimulation across the entire epicardium. *Nature Commun.* **5,** 3329 (2014).
14. Mannsfeld, S. C. B. *et al.* Highly sensitive flexible pressure sensors with microstructured rubber dielectric layers. *Nature Mater.* **9,** 859–864 (2010).
15. Someya, T. *et al.* Conformable, flexible, large-area networks of pressure and thermal sensors with organic transistor active matrixes. *Proc. Natl Acad. Sci. USA* **102,** 12321–12325 (2005).
16. Wang, C. *et al.* User-interactive electronic skin for instantaneous pressure visualization. *Nature Mater.* **12,** 899–904 (2013).
17. Pan, L. *et al.* An ultra-sensitive resistive pressure sensor based on hollow-sphere microstructure induced elasticity in conducting polymer film. *Nature Commun.* **5,** 3002 (2014).
18. Takei, K. *et al.* Nanowire active-matrix circuitry for low-voltage macroscale artificial skin. *Nature Mater.* **9,** 821–826 (2010).
19. Schwartz, G. *et al.* Flexible polymer transistor with high pressure sensitivity for application in electronic skin and health monitoring. *Nature Commun.* **4,** 1859 (2013).
20. Gong, S. *et al.* A wearable and highly sensitive pressure sensor with ultrathin gold nanowires. *Nature Commun.* **5,** 3132 (2014).
21. Dagdeviren, C. *et al.* Conformable-amplified lead zirconate titanate sensors with enhanced piezoelectric response for cutaneous pressure monitoring. *Nature Commun.* **5,** 4496 (2014).
22. Sekitani, T. *et al.* Stretchable active-matrix organic light-emitting diode display using printable elastic conductors. *Nature Mater.* **8,** 494–499 (2009).
23. Fukushima, T. *et al.* Molecular ordering of organic molten salts triggered by single-walled carbon nanotubes. *Science* **300,** 2072–2074 (2003).

24. Bhardwaj, N. & Kundu, S. C. Electrospinning: a fascinating fiber fabrication technique. *Biotechnol. Adv.* **28,** 325–347 (2010).
25. Kim, T. *et al.* Injectable, cellular-scale optoelectronics with applications for wireless optogenetics. *Science* **340,** 211–216 (2013).
26. Kaltenbrunner, M. *et al.* An ultra-lightweight design for imperceptible plastic electronics. *Nature* **499,** 458–463 (2013).
27. Lee, S. *et al.* A strain-absorbing design for tissue–machine interfaces using a tunable adhesive gel. *Nature Commun.* **5,** 5898 (2014).
28. Gibson, L. J. & Ashelby, M. F. *Cellular Solids: Structure and Properties* (Cambridge Univ. Press, 1999).

Acknowledgements

This work was supported by a Japan Science and Technology Agency (JST) Someya Bio-Harmonized ERATO grant. The authors thank W. Yukita and B. Hwang for supporting the experiment.

Author contributions

Sungwon L., A.R., J.R., Sunghoon L., H.J. and T.So. performed the device design and fabrication. T.Y., T.I. and Y.A. performed electric and structural characterization of devices. Q.L. and Z.S. performed numerical analysis of the strain. T.Y. contributed the material analysis tools. T.Se helped with material design and fabrication. Sungwon L., A.R., J.R. and T.So. discussed and prepared the manuscript with input from all co-authors. T.So. supervised the project.

Additional information

Supplementary information is available in the online version of the paper. Reprints and permissions information is available online at www.nature.com/reprints. Correspondence and requests for materials should be addressed to T.S.

Competing financial interests

The authors declare no competing financial interests.

Methods

Pressure-sensitive nanofibre fabrication. The following materials were mixed and stirred for 5 h with 4-methyl-2-pentanone (3 g): 2 g fluorinated copolymer, vinylidenefluoride-tetrafluoroethylene-hexafluoropropylene (Daikin, G912), 0.2 g ionic liquid (1-butyl-3methylimidazolium bis(trifluoromethanesulphonyl)imide, 0.6 g graphene (dispersed in 4-methyl-2-pentanone at 10 wt% using jet milling at 10 MPa for ten passes) and 0.6 g CNTs (dispersed in the same solvent at 0.1 wt% using jet milling at 10 MPa for ten passes). The solution was then deposited using electrospinning. The feed rate was 2 μl min^{-1}, the voltage was 15 kV and the distance between the substrate and syringe was 25 cm.

Pressure response, reversibility and transmittance measurement. Pressure-sensitive fibres were deposited on a PET substrate with a 1 cm^2 Au pad. The fibres were then sandwiched by an identical electrode. The electrical properties were measured using an *I*–*V* parameter analyser (Agilent, 4156C) while applying pressure. For the cyclic test, a dynamic mechanical analyser from Shimadzu (AG-X) was used. A weight was suspended above the sample. The movement speed was 5 mm s^{-1} with a holding time of 0.5 s. The transmittance was measured using an ellipsometer (J.A. Woollam, M-2000).

Bending test of the sensor and measurement of the pressure response in the bent state. The pressure-sensor devices were fabricated on different substrates. PI films with thicknesses of 75 and 12.5 μm (UPILEX 75S, Ube Industrial) and a 1.4-μm-thick PET foil (Mylar 1.4 CW02, Pütz) were used. For the device deposited on a 1.4-μm-thick PET foil, we deposited an additional fluorinated copolymer for 3 min to adjust the sensitivity to be the same as that of the device fabricated on a thicker substrate (>10 μm). Each device was bent between two plates while the distance was decreased. The bending radius of the sensor was calculated using camera images and photo-analysis software. The sensors were completely folded until their bending radii reached ~180 μm and were then slowly released. During this process, their electrical properties were measured. The pressure sensor fabricated on the 1.4-μm-thick PET substrate was attached to metal bars with different bending radii. The sensor was then pressed by a small stainless-steel stick (0.8 or 3.2 g) to apply pressure. The length and outer diameter of the stick were 5 and 0.8 cm, respectively.

Fabrication of a transparent pressure-sensor array and e-skin demonstration. The sensor array was fabricated on a 1.4-μm-thick PET film supported by a polymer layer. A layer of indium tin oxide (ITO, 30 nm) was deposited and patterned as a bottom electrode using sputtering. The width and length of the ITO pattern were 5 mm and 8 cm, respectively, and the distance between the patterns was 5 mm. A pressure-sensitive nanofibre layer was then deposited (2 min of deposition; all other conditions were the same as those used for nanofibre fabrication). The top ITO electrode was prepared in the same manner. Finally, the top electrode covered the nanofibre layer with an ITO pattern in a direction that was perpendicular to the bottom electrode. Cu wires were connected using a small amount of Ag paste.

Integration with active matrix. A 1-μm-thick parylene substrate was prepared by chemical vapour deposition on a wafer. A 20-nm-thick Au layer was evaporated as a gate. A 200-nm-thick parylene layer was then formed as a gate insulator. The gate dielectric had a capacitance of 13.7 nF cm^{-2}. A 30-nm-thick dinaphtho[2,3-*b*:2′,3′-*f*]thieno[3,2-*b*]thiophene (DNTT) organic active layer was deposited by evaporation. A 50-nm-thick Au layer was deposited to form the source, drain and interconnection, and a 1-μm-thick layer of parylene was deposited for encapsulation. A via hole was drilled using a laser. Finally, Au was deposited to establish a connection with the pressure-sensor layer. The pressure-sensor sheet was fabricated on a 1.4-μm-thick PET film, and this pressure sensor was connected to ground.

Measurement of pressure and its propagation on an artificial blood vessel. Sensors (2 min of deposition time and a pad size of 2 × 4 mm^2) were fabricated on a 1.4-μm-thick PET film. The sensors were attached to the artificial blood vessel model (a silicone tube from Shin-Etsu Chemical Co., with inner and outer diameters of 16 and 18 mm, respectively, which are comparable to those of a human aorta) and wrapped with a plastic film. Water pressure was applied using a displacement-type artificial heart (Nippon Zeon, Zeon pump) controlled by a console (Aisin Seiki, Corart; 0–100 mmHg, 2 beats per second). The current response to the pressure was measured using an applied voltage of 1 V. Pressure propagation was measured using an oscilloscope (Agilent, DOS6054A) for better time resolution (0.5 ms). Each pressure sensor was connected in series to a resistor (1.5 MΩ), and voltage was applied (1 V) using a function generator (Texio, FG-281). An initial pressure was applied to each sensor (100 Pa, which corresponds to 100 MΩ) for calibration by wrapping the outer thin film until the resistance of each sensor became 100 MΩ.